MultiScience - XXX. microCAD International Multidisciplinary Scientific Conference
University of Miskolc, Hungary, 21-22 April 2016, ISBN 978-963-358-113-1

SIMULATION OF PROCESS PARAMETERS TOWARDS THE GENERATION OF LOW SPATIAL FREQUENCY LIPSS ON DIELECTRIC MATERIALS

Simon Schwarz[1], Stefan Rung[2], Ralf Hellmann[3]
[1] B. Eng., Master student
[2] M. Eng., Ph. D. student
[3] Prof. Dr., Head of applied laser and photonics group
[1,2,3] Applied laser and photonics group, University of Applied Sciences Aschaffenburg, 63743 Aschaffenburg, Germany

ABSTRACT

In this paper we show simulations of low spatial frequency laser-induced period surface structures (LSFL) and deduce appropriate process parameters for their specific experimental generation on dielectrics. We employed the established efficacy factor theory to forecast the periodicity and the orientation of low spatial frequency laser-induced period surface structures including a Drude-model to determine the required carrier density for LSFL generation. This approach is applied exemplarily to the LSFL generation on fused silica. We extend the theoretical approach by a rate equation based calculation of the required laser fluence to excite the necessary carrier density by photo- and avalanche ionization using ultra-short pulsed laser irradiation.

INTRODUCTION

Laser-induced periodic surface structures (LIPPS) are a universal phenomenon after irradiation of solid materials with polarized laser light (see figure 1). LIPPS were firstly reported by Birnbaum [1] and have been intensively studied during recent years being found on conductors [2-4], semiconductors [1,2,5] and dielectrics [2,6,7]. Two types of LIPSS are generally distinguished: low spatial frequency LIPSS (LSFL) and high spatial frequency LIPSS (HSFL). The difference between these two types is the periodicity Λ of the periodic structures and the orientation with respect to each other being orthogonal. For LSFL, Λ_{LSFL} is in the range of the laser wavelength λ whereas Λ_{HSFL} is smaller than $\lambda/2$ [2]. Emmony et al. [8] established a fundamental theory for LSFL wherein the basic approach is based on interference between the incident laser light and a scattered wave on the rough surface. The period Λ_{LSFL} is determined to be $\lambda/(1 \pm sin\Theta)$, with Θ being the angle of incidence. Sipe et al. [9] further developed this theoretical approach and established a mathematical formalism for the interference of the incident laser light with a surface scattered wave. Contrary to this, for HSFL no established model exists yet.

DOI: 10.26649/musci.2016.016

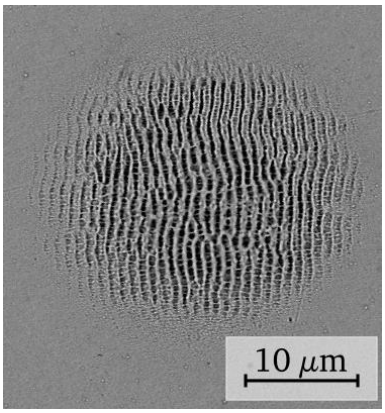

Fig. 1
Scanning electron microscope image of LSFL on stainless steal

For dielectric materials, the development of surface scattered waves is more challenging due to the absence of free and the difficulty to generate them above the band gap. However, LIPSS generation on dielectric materials, such as fused silica, is highly attractive, since manifold applications of these materials would benefit from the possibility to alter the wettability properties e.g. for microfluidics [3,4] or the cell growth in biotechnical applications [7,10] by the periodic surface structures.

THEORETICAL BASIS FOR SIMULATION

The first established theory about the generation of LSFL was introduced in the 1973 by Emmony et al. [8], attributing their generation to an interference between the incident laser light with a scattered wave on the rough surface. Based on this approach, 1983 Sipe et al. [9] composed a mathematical formalism to simulate the inhomogeneous energy deposition of the irradiated laser light interfering with a surface scattered wave at a rough surface (generally referred to the efficacy factor (EF) theory). Eq. 1 describes the inhomogeneous energy deposition $A(\vec{k})$ while $b(\vec{k})$ is the Fourier component of the rough surface and $\eta(\vec{k}, \vec{k}_i)$ the efficacy factor, with $\vec{k}_i$ describing the wave vector component of the incident laser and $\vec{k}$ the wave vector, both parallel to the surface. While $b(\vec{k})$ is a slowly changing function, only $\eta(\vec{k}, \vec{k}_i)$ is generally under investigation to calculate the orientation and periodicity of appearing LSFL.

$$A(\vec{k}) \propto \eta(\vec{k}, \vec{k}_i)\, |b(\vec{k})| \tag{1}$$

In Eq. 2 the efficacy factor is shown with the expressions $\nu(\vec{k}_+)$ and $\nu^*(\vec{k}_-)$ as auxiliary functions. Within this approach, $\eta(\vec{k}, \vec{k}_i)$ depends on the laser wavelength, angle of incidence, complex refractive index, surface topography and the polarization of the laser light [9]. Simulating $\eta(\vec{k}, \vec{k}_i)$ yields the efficacy to create LSFL, their periodicity and orientation.

$$\eta(\vec{k}, \vec{k}_i) = 2\pi \, |\nu(\vec{k}_+) + \nu^*(\vec{k}_-)\,| \tag{2}$$

Upon irradiation of dielectrics with ultra-short pulsed lasers having high peak intensities I_0, the materials change their characteristics. Free charge carriers are excited while and after the laser pulse, causing changes in the complex dielectric permittivity. In case of fused silica, which is investigated here, this is equivalent to a change of the complex refractive index with $\tilde{\varepsilon}$ being the complex permittivity of the non-excited material and $\tilde{n}$ the complex refractive index ($\tilde{\varepsilon} = \tilde{n}^2$) [11]. Applying a Drude-model, Dufft et al. [11] calculated the complex refractive index change ($\Delta\tilde{\varepsilon}_{Drude}$) including different excited states. As a result, $\Delta\tilde{\varepsilon}_{Drude}$ is given by equation 3, including the electron charge e, the laser-induced free carrier density N_e, the vacuum dielectric permittivity ε_0, the optical effective mass of the electrons m^*_{opt}, the free electron mass m_e, the optical angular frequency ω and the Drude damping time τ_D, respectively.

$$\Delta\tilde{\varepsilon}_{Drude} = \frac{-e^2 N_e}{\varepsilon_0 m^*_{opt} m_e \omega^2 [1 + \frac{i}{\omega\tau_D}]} \tag{3}$$

Stuart et al. calculated N_e based on a rate equation including the processes photo- and avalanche ionization [12]. Equation 4 expresses the evolution of the carrier density with the avalanche coefficient α and the time dependent laser intensity $I(t)$ yielding the avalanche ionization. The photoionization is given by a strong-field Keldysh formula $P(I)$.

$$\frac{\partial N_e}{\partial t} = \alpha I(t) N_e + P(I) \tag{4}$$

In this contribution, we apply the above described combined EF theory / Drude-model approach to determine the required carrier density for LSFL generation with a specified periodicity and orientation. In a second step, we calculate the necessary laser fluence Φ_0 for an ultra-short pulsed laser to excite this required carrier density in fused silica by photo- and avalanche ionization. This provides a practical guide for the specific generation of LSFL with defined periodicity and orientation.

SIMULATION OF EFFICACY FACTOR

Simulation of the EF for fused silica with different excitation states have been done under laser irradiation with a wavelength of λ = 1030 nm and an angle of incidence Θ = 0°. The complex refractive index of fused silica is taken from Ref. 13 to be n = 1.45 + i0 at a non-excited state. Further parameters for simulation can be found in table 1.

Table 1
Parameters used for simulation of EF

Symbol	Description	Value	Reference
λ	wavelength	1030 nm	
Θ	angle of incidence	0°	
p	polarization	p-pol	
n	complex refractive index	1.45 + i0	[13]
m_{opt}^{*}	effective mass of electrons	0.86	[14]
τ_D	Drude damping time	1.0 fs	[14]
f	filling factor	0.1	[5,9]
s	shape factor	0.4	[5,9]

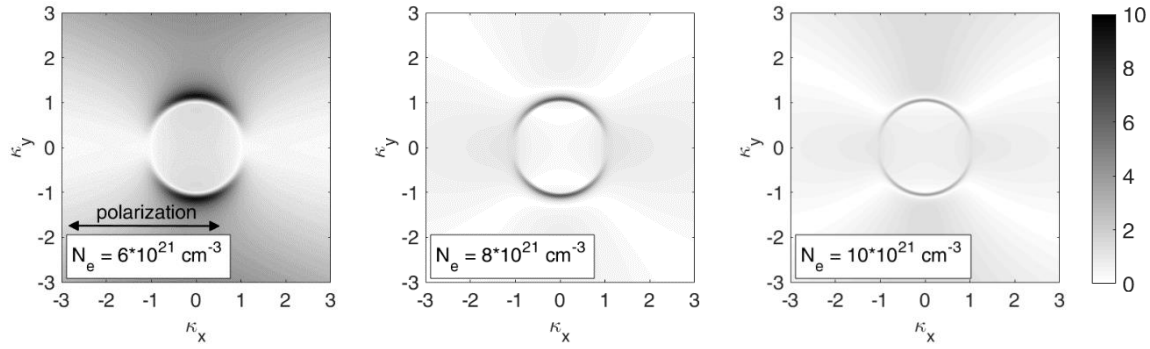

Fig. 2
EF maps for different excited states of fused silica showing $\eta(\vec{k},\vec{k}_i)$ in the Fourier space of $\kappa_x = \lambda/\Lambda_{LSFL}$ in normalized colour map

Figure 2 shows different resulting EF maps in a normalized colour map style. The efficacy factor is given in the Fourier space with $\kappa_{x,y}$ being λ/Λ_{LSFL}. The EF maps are showing sickle-shaped features typical for LSFL. According to Sipe et al. and Young et al. [5, 9], LSFL are not only formed where the efficacy factor $\eta(\vec{k},\vec{k}_i)$ reaches high values, but also where the efficacy factor exhibits distinct sharp peaks. We therefore analyse cross sections of the different efficacy factor maps. Taking into account the orientation of the typical sickle-shaped features in the EF maps, we orientate the cross sections along $\kappa_x = 0$ and $\kappa_y = 0$ as shown in figure 3 for different carrier densities. It turns out that cross sections for $\kappa_y = 0$ aren't of interest because $\eta(\vec{k},\vec{k}_i)$ remains on a significantly lower level as compared to those for $\kappa_x = 0$. Apparently, the efficacy factor becomes largest for a carrier density of N_e = 6*10^{21} cm^{-3} at $\kappa_x = 0$. However, for lower carrier densities sharper peaks within the cross section are perceived. As a trade-off between distinct peaks and high values of EF in the cross sections, we choose a carrier density of N_e = 8*10^{21} cm^{-3} as an appropriate compromise for the further examination. For this carrier density, the two sickle-shaped features in figure 2 indicate the orientation of the LSFL parallel to the polarization of the laser (the later indicated by the black arrow in Fig. 2). In addition, for this carrier density figure 3 yields a periodicity of the LSFL ($\Lambda_{LSFL} = \lambda/\kappa_y$) of 954 nm.

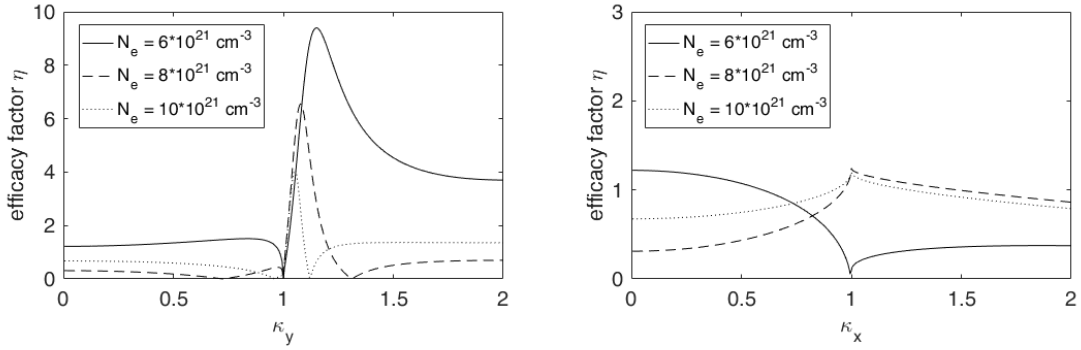

Fig. 3
Cross section of EF maps for different carrier densities N_e at κ_x = 0 (left) and κ_y = 0 (right).

CALCULATION OF FREE CHARGE CARRIERS

After identifying a suitable carrier density (here N_e = 8*10^{21} cm^{-3}) to generate LSFL with specified properties (periodicity and orientation), we determine the required laser fluence to excite this chosen carrier density by photo- and avalanche ionization by solving the rate equation given in formula 4. Since fused silica has a band gap of 9 eV [16], an eight-photon-absorption is necessary to excite carriers with a wavelength of 1030 nm. The avalanche coefficient α is taken to be 0.01 cm² ps^{-1}/GW [12] and for the photoionization $P(I)$ = 9.52*10^{10}*I^8 cm^{-3} ps^{-1} is used [16]. Based on the employed laser parameters wavelength $\lambda = 1030$ nm and laser pulse width τ = 222 fs (FWHM), our calculations reveal that a carrier density of N_e = 8*10^{21} cm^{-3} can be excited after the laser pulse with a peak intensity I_0 = 7.6 TW/cm^2. This intensity corresponds to a peak fluence Φ_0 of 1.8 J/cm^2 ($\Phi_0 = (\pi/ln2)^{0.5}\, I_0\, \tau/2$), which is in good agreement to those values determined by Stuart et al. for similar laser parameters [16]. In addition, these findings confirm that the generation of LSFL occurs in a fluence range close to the ablation threshold of the material [2, 3].

CONCLUSION

We applied the efficacy factor theory extended by a Drude-model and simulated the required carrier density to generate laser-induced periodic surface structures with low spatial frequency on fused silica. Based on a rate equation including photo- and avalanche ionization we further extended the theoretical approach to calculate the necessary laser fluence to excite the afore determined carrier density. For exemplarily chosen laser parameters of 1030 nm wavelength and 220 fs pulse width, the simulations yield a periodicity of Λ_{LSFL} = 954 nm and an orientation parallel to the incident laser light. Moreover, the extended calculation of the laser fluence provides a practical guide to generate these LSFL. Further experiments will be conducted and presented to experimentally prove this extended concept.

REFERENCES

[1] BIRNBAUM, M.: **Semiconductor Surface Damage Produced by Ruby Lasers**. **-** Journal of Applied Physics 36, 1965. 3688.

[2] BONSE, J., KRÜGER, J., HÖHM, S., AND ROSENFELD**,** A.: **Femtosecond laser-induced periodic surface structures. -** Journal of Laser Applications 24, 2012. 042006.

[3] CUNHA, A., SERRO, A. P., OLIVEIRA, V., ALMEIDA, A., VILAR, R., AND DURRIEU, M.-C.: **Wetting behaviour of femtosecond laser textured Ti-6Al-4V surfaces. –** Applied Surface Science 265, 2013. p. 688-696.

[4] JAGDHEESH, R., PATHIRAJ, B., KARATAY, E., RÖMER, G. R. B. E., AND HUIS IN'T VELD, A. J**.: Laser-Induced Nanoscale Superhydrophobic Structures on Metal Surfaces. -** Langmuir: the ACS journal of surfaces and colloids 27, 2011. p. 8464-8469.

[5] YOUNG, J. F., PRESTON, J. S., VAN DRIEL, H. M., AND SIPE, J. E.: **Laser-induced periodic surface structure. II. Experiments on Ge, Si, Al, and Brass. -** Physical Review B 27, 1983. p. 1155-1172.

[6] ROHLOFF, M., DAS, S. K., HÖHM, S., GRUNWALD, R., ROSENFELD, A., KRÜGER, J., AND BONSE, J.: **Formation of laser-induced periodic surface structures on fused silica upon multiple cross-polarized double-femtosecond-laser-pulse irradiation sequences. -** Journal of Applied Physics 110, 2011. 014910.

[7] REBOLLAR, E., FRISCHAUF, I., OLBRICH, M., PETERBAUER, T., HERING, S., PREINER, J., HINTERDORFER, P., ROMANIN, C., AND HEITZ, J.: **Proliferation of aligned mammalian cells on laser-nanostructured polystyrene. -** Biomaterials 29, 2008. p. 1796-1806.

[8] EMMONY, D. C, HOWSON, R. P., AND WILLIS, L. J..: **Laser mirror damage in germanium at 10.6 µm. -** Applied Physics Letters 23, 1973. p. 598-600.

[9] SIPE, J. E., YOUNG, J. F., PRESTON, J. S., AND VAN DRIEL, H. M.: **Laser-induced periodic surface structure. I. Theory. -** Physical Review B 27, 1983. p. 1141-1154.

[10] WALLAT, K., DÖRR, D., LE HARZIC, R., STRACKE, F., SAUER, D., NEUMEIER, M., KOVTUN, A., ZIMMERMANN, H., AND EPPLE, M.: **Cellular reactions toward nanostructured silicon surfaces created by laser ablation. -** Journal of Laser Applications 24, 2012. 042016.

[11] DUFFT, D., ROSENFELD, A., DAS, S. K., GRUNDWALD, R., BONSE, J.: **Femtosecond laser-induced periodic surface structures revisited: a comparative study on ZnO. –** Journal of Applied Physics 105, 2009. 034908.

[12] STUART, B. C., FEIT, M. D., RUBENCHIK, A. M., SHORE, B. W., AND PERRY, M. D.: **Laser-Induced Damage in Dielectrics with Nanosecond to Subpicosecond Pulses. -** Physical Review Letters 74, 1995. p. 2248-2251

[13] MALITSON, I. H.: **Interspecimen Comparison of the Refractive Index of Fused Silica. -** Journal of the Optical Society of America 55, 1965. p. 1205-1209.

[14] WU, A. Q., CHOWDHURY, I. H., AND XU, X.: **Femtosecond laser absorption in fused silica: Numerical and experimental investigation. -** Physical Review B 72, 2005. 085128

[15] BONSE, J., MUNZ, M., AND STURM, H.: **Structure formation on the surface of indium phosphide irradiated by femtosecond laser pulses. -** Journal of Applied Physics 97, 2005. 013538.

[16] STUART, B. C., FEIT, M. D., HERMAN, S., RUBENCHIK, A. M., SHORE, B. W., AND PERRY, M. D.: **Nanosecond-to-femtosecond laser-induced breakdown in dielectrics. -** Physical Review B 53, 1996. p. 1749-1761.

[17] TIEN, A.-C., BACKUS, S., KAPTEYN, H., MURNANE, M., AND MOUROU, G.: **Short-Pulse Laser Damage in Transparent Materials as a Function of Pulse Duration. –** Physical Review Letters 82, 1999. p. 3883-3886.

[18] ROSENFELD, A., LORENZ, M., STOIAN, R., AND ASHKENASI, D.: **Ultrashort-laser-pulse damage threshold of transparent materials and the role of incubation. -** Applied Physics A: Materials Science & Processing 69, 1999. p. 373-376.

[19] VAREL, H., ASHKENASI, D., ROSENFELD, A., HERRMANN, R., NOACK, F., CAMPBELL, E. E. B.: **Laser-induced damage in SiO2 and CaF2 with picosecond and femtosecond laser pulses. –** Journal of Applied Physics 62, 1996. p. 293-294.

[20] LIU, J. M.: **Simple technique for measurements of pulsed Gaussian-beam spot sizes. -** Optics Letters 7, 1982. 196-198.

[21] HÖHM, S., ROSENFELD, A., KRÜGER, J., AND BONSE, J.: **Femtosecond laser-induced periodic surface structures on silica. -** Journal of Applied Physics 112, 2012. 014901.